



1 **Revised treatment of wet scavenging processes dramatically improves GEOS-Chem**
2 **12.0.0 simulations of nitric acid, nitrate, and ammonium over the United States**

3

4 Gan Luo, Fangqun Yu, and James Schwab

5 Atmospheric Sciences Research Center, University at Albany

6

7 **Abstract**

8 The widely used community model GEOS-Chem 12.0.0 and previous versions have
9 been recognized to significantly overestimate the concentrations of gaseous nitric acid,
10 aerosol nitrate, and aerosol ammonium over the United States. The concentrations of
11 nitric acid are also significantly over-predicted in most global models participating a
12 recent model inter-comparison study. In this study, we show that most or all of this
13 overestimation issue appears to be associated with wet scavenging processes.
14 Replacement of constant in-cloud condensation water (ICCW) assumed in GEOS-Chem
15 standard versions with one varying with location and time from the assimilated
16 meteorology significantly reduces mass loadings of nitrate and ammonium during the
17 wintertime, while the employment of an empirical washout rate for nitric acid
18 significantly decreases mass concentrations of nitric acid and ammonium during the
19 summertime. Compared to the standard version, GEOS-Chem with updated ICCW and
20 washout rate significantly reduces the simulated annual mean mass concentrations of
21 nitric acid, nitrate, and ammonium at surface mentoring network sites in US, from 2.04 to
22 $1.03 \mu\text{g m}^{-3}$, 1.89 to $0.88 \mu\text{g m}^{-3}$, 1.09 to $0.68 \mu\text{g m}^{-3}$, respectively, in much better
23 agreement with corresponding observed values of 0.83, 0.70, and $0.60 \mu\text{g m}^{-3}$,
24 respectively. In addition, the agreement of model simulated seasonal variations of
25 corresponding species with measurements is also improved. The updated wet scavenging
26 scheme improves the skill of the model in predicting nitric acid, nitrate, and ammonium
27 concentrations which are important species for air quality and climate.



1 **1. Introduction**

2 Nitrate and ammonium are important secondary inorganic aerosols in the
3 atmosphere, contributing significantly to total aerosol mass over most polluted regions
4 (Bian et al., 2017) and to aerosol direct radiative forcing over urban and agriculture
5 regions (Bauer et al., 2007; Myhre et al., 2013). The amount of nitrate and ammonium
6 also regulates the concentration of gaseous ammonia which often plays an important role
7 in the formation of new particles (Kirkby et al., 2011; Yu et al., 2018). In addition, nitrate
8 and ammonium help newly formed particles grow to larger sizes suitable for cloud
9 condensation nuclei (Yu and Luo, 2009) and thus can impact aerosol indirect radiative
10 forcing (Twomey, 1977).

11 Nitric acid, nitrate, and ammonium concentrations are often overestimated by
12 atmospheric models (Pye et al., 2009; Walker et al., 2012; Bian et al., 2017; Zakoura and
13 Pandis, 2018), including the widely used community model GEOS-Chem (e.g., Zhang et
14 al., 2012; Heald et al., 2012). Zhang et al. (2012) studied nitrogen deposition over the US
15 with GEOS-Chem and found both nitric acid and nitrate concentrations are overestimated,
16 especially in wintertime. They suggested that this is the result of excessive nitric acid
17 formation via night time chemistry of heterogeneous N_2O_5 hydrolysis. However, Heald et
18 al. (2012) found the overestimate of heterogeneous N_2O_5 hydrolysis does not fully
19 account for the nitrate bias and suggested the positive nitrate bias is likely linked with an
20 overestimate of nitric acid concentrations. Heald et al. (2012) investigated other possible
21 causes for the overestimation of nitric acid concentrations arising from uncertainties in
22 daytime formation and dry deposition, and concluded that none of these uncertainties
23 could fully account for the reduction in nitric acid required to correct the nitrate bias.
24 Based on comparisons of simulated nitrate and ammonium aerosol from nine
25 AEROCOM models with ground station and aircraft measurements, Bian et al. (2017)
26 concluded that most models overestimate surface nitric acid volume mixing ratio by a
27 factor of up to 3.9 over North America and the overestimation cannot be simply attributed



1 to model uncertainties. Backes et al. (2016) suggested that uncertainties in the temporal
2 profiles of ammonia emissions could also contribute significantly to the bias of nitrate
3 concentrations. However, the impact of ammonia mostly happened during summer time.
4 Zakoura and Pandis (2018) found significant decrease in nitrate concentration when they
5 enhanced their model resolution from 36 km × 36 km to 4 km × 4 km in the PMCAMx
6 model. However, similar results are not found in global models with much coarser grids
7 than regional models. All these studies indicate that the overestimation of nitric acid,
8 nitrate, and ammonium mass concentrations in current atmospheric chemistry models
9 remains to be resolved.

10 In this study, we proposed an improved treatment of wet scavenging in GEOS-Chem
11 by considering cloud condensation water variability and empirical washout rate, which
12 together significantly improve the estimates of nitric acid, nitrate, and ammonium over
13 the US. The improved wet scavenging in GEOS-Chem is described in section 2. The
14 comparison of model results with in-site observations and the changes of the three
15 species over the US are presented in section 3. Section 4 is the summary and discussion.

16

17 **2. Improved scheme for wet scavenging**

18 Wet scavenging is the main removal pathway for many atmospheric air pollutants.
19 Two mechanisms are involved in wet scavenging: rainout (in-cloud scavenging) and
20 washout (below-cloud scavenging). GEOS-Chem treats wet scavenging associated with
21 stratiform and convective precipitation separately.

22

23 **2.1 Impact of in cloud condensed water (ICCW)**

24 For stratiform precipitation, in the most recently released GEOS-Chem version
25 12.0.0 (GC12), rainout is parameterized according to Jacob et al. (2000) as

$$26 \quad F = \frac{P_r}{k \cdot ICCW} (1 - e^{-k \cdot \Delta t}) \quad (1)$$

27 where F is the fraction of a soluble tracer in the grid-box scavenged by rainout, Δt is the



1 model integration time step. k is the first-order rainout loss rate which represents the
2 conversion of cloud water to precipitation water. $ICCW$ represents the condensed water
3 content (liquid) within the precipitating cloud (i.e., in cloud) and P_r is the rate of new
4 precipitation formation in the corresponding grid-box.

5 The rainout loss rate (k) represents how fast cloud condensation water can be
6 removed from the atmosphere and thus is critical for rainout scavenging. k is defined in
7 Jacob et al. (2000) and coded in GC12 (called k_{GC12} thereafter) as

$$8 \quad k_{GC12} = k_{min} + \frac{P_r}{ICCW} \quad (2)$$

9 where k_{min} is the minimum value of rainout loss rate derived from the stochastic
10 collection equation which indicates that in one hour at least ~ 0.36 of cloud droplets are
11 lost to autoconversion/accretion (Beheng and Doms 1986). In GC12, k_{min} is set to be 0.36
12 $\text{hr}^{-1} = 1 \times 10^{-4} \text{ s}^{-1}$.

13 It should be noted that P_r in Eq. (2) is a grid-box mean value, while $ICCW$ is an
14 cloud value. To be physically consistent, we suggest a new expression of k (k_{new}) that
15 replaces grid-box mean P_r with the corresponding in cloud value P_r/f_c .

$$16 \quad k_{new} = k_{min} + \frac{P_r}{f_c \cdot ICCW} \quad (3)$$

17 where f_c is the grid-box mean cloud fraction. As we will show later, Eq. (3) gives k values
18 in much better agreement with those derived from cloud model simulations and
19 observations.

20 To calculate F , GC12 uses P_r from the Modern-Era Retrospective analysis for
21 Research and Applications Version 2 (MERRA2) meteorological fields. For $ICCW$ in Eqs.
22 1-3, Jacob et al. (2000) used a constant value of 1.5 g m^{-3} and Wang et al. (2011) changed
23 it to 1 g m^{-3} . In GC12, the default value of $ICCW$ is 1 g m^{-3} . However, $ICCW$ in the
24 atmosphere varies with time and location. Here we suggest to use time and location
25 dependent $ICCW$ (named $ICCW_t$) which can be derived from MERRA2 meteorological
26 fields as



1
$$ICCW_t = \frac{CW + P_r \cdot \Delta t}{f_c} \quad (4)$$

2 where CW is grid-box mean cloud water content, while $P_r \cdot \Delta t$ represents rain water
3 content produced during the time step Δt .

4 Figure 1a shows seasonal variations of $ICCW_t$ (Eq. 4) averaged throughout the lower
5 troposphere (0–3 km) of the whole globe ($ICCW_{t,G}$), over all land surface ($ICCW_{t,L}$),
6 over the oceans ($ICCW_{t,O}$), and over the continental US ($ICCW_{t,US}$). For comparisons, the
7 constant values of $ICCW$ assumed in Jacob et al. (2000) ($ICCW_{J2000}$) and GC12
8 ($ICCW_{GC12}$) are also shown. The monthly mean values of $ICCW_{t,G}$, $ICCW_{t,L}$, $ICCW_{t,O}$,
9 and $ICCW_{t,US}$ vary within the ranges of 0.90–1.03 g m⁻³, 0.30–0.45 g m⁻³, 1.15–1.26 g
10 m⁻³, and 0.21–0.53 g m⁻³, respectively. This figure shows that $ICCW_{t,G}$ is close to the
11 assumed $ICCW$ value of 1 g m⁻³ used in GC12. As can be seen from Fig. 1a, $ICCW_{t,O}$ is
12 greater than 1 g m⁻³, but $ICCW_{t,L}$ is much less than the constant value of 1 g m⁻³ assumed
13 in GC12. The mean $ICCW$ over the continental US (bright green line) is close to $ICCW_{t,L}$
14 (olive line), and is ~ 5 times less than the assumed value in GC12 during the wintertime
15 and ~ 2 times less during the summertime. As we will show later, the constant $ICCW$ of 1
16 g m⁻³ assumed in GC12 leads to significant underestimation of rainout over the
17 continental US, especially during the wintertime.

18 Figure 1b shows seasonal variations of mean k_{GC12} , k_{new} , and $k_{new_ICCW_t}$ in the lower
19 troposphere (0–3 km) of the continental US. Referring to Eq. (2), the figure shows that
20 k_{GC12} is dominated by k_{min} (which is physically unsound) and thus shows negligible
21 seasonal variation. Conversely, k_{new} is low in the wintertime and high in the
22 summertime. $k_{new_ICCW_t}$ is 2.3 times higher than k_{new} during January and 1.6 times higher
23 than k_{new} during July. Both k_{new} and $k_{new_ICCW_t}$ are within the range of rainout loss rates
24 (10^{-4} – 10^{-3} s⁻¹) indicated by cloud model simulations and estimates based on observations
25 (Giorgi and Chameides, 1986).



1 From Eqs. (1), (3), and (4), we can get the updated parameterization for rainout loss
2 fraction at each location and time step

$$3 \quad F = \frac{f_c \cdot P_r}{k_{new_ICCW_t} (CW + P_r \cdot \Delta t)} \left(1 - e^{-k_{new_ICCW_t} \Delta t} \right) \quad (5)$$

4

5 **2.2 Impact of empirical washout rate on nitric acid wet scavenging**

6 Still considering the case of stratiform precipitation in GOES-Chem, the fraction of
7 aerosols and HNO₃ within a grid-box that is scavenged by washout over a time step is
8 parameterized as (Wang et al., 2011; Liu et al., 2001; Jacob et al., 2000)

$$9 \quad F_{wash} = f_r (1 - \exp(-k_{wash} \Delta t)) \quad (6)$$

$$10 \quad f_r = \max\left(\frac{P_r}{k \cdot ICCW}, f_{top}\right) \quad (7)$$

$$11 \quad k_{wash} = \Lambda \left(\frac{P_r}{f_r}\right)^b \quad (8)$$

12 where f_r is the horizontal areal fraction of the grid-box experiencing precipitation and f_{top}
13 is the value of f_r in the layer overhead ($f_{top} = 0$ at the top of the precipitating column).
14 k_{wash} is washout rate, Λ is washout scavenging coefficient, and b is an exponential
15 coefficient. In the original GEOS-Chem, $\Lambda = 1 \text{ cm}^{-1}$ and $b = 1$ for both aerosols and nitric
16 acid (Liu et al., 2001; Jacob et al., 2000).

17 It has been well recognized that, for aerosols, Λ and b depend on particle size (Wang
18 et al., 2010; Feng, 2007; Andronache et al., 2006; Henzing et al., 2006; Laakso et al.,
19 2003). Feng (2007) suggested values of $b = 0.62$, 0.61 , and 0.8 for particles in nucleation
20 (diameter $1 \text{ nm} - 40 \text{ nm}$), accumulation ($40 \text{ nm} - 2.5 \text{ }\mu\text{m}$), and coarse mode ($>2.5 \text{ }\mu\text{m}$),
21 respectively. Many studies indicate that there are large difference between existing
22 theoretical and observed size-resolved washout rates (Wang et al., 2010; Andronache et
23 al., 2006; Henzing et al., 2006; Laakso et al., 2003). For particles within the diameter
24 range of $0.01 - 2 \text{ }\mu\text{m}$, size-resolved washout rates derived from analytical formulas are one
25 to two orders of magnitude smaller than those derived from field measurements (e.g.,



1 Wang et al., 2010). This large difference could result from turbulent flow fluctuations
2 (Andronache et al. 2006; Khain and Pinsky, 1997), vertical diffusion process (Zhang et al.,
3 2004), and droplet-particle collection mechanisms (Park et al., 2005).

4 In GC12, Λ and b for aerosols are parameterized as a function of particle size modes
5 (Wang et al., 2011), following Feng (2007). For nitric acid, GC12 keeps $\Lambda = 1 \text{ cm}^{-1}$ and b
6 $= 1$, unchanged from the original CEOS-Chem parameters. In this study, we employ the
7 size-dependent aerosol washout parameterization derived from six years of field
8 measurements over forests in southern Finland (Laakso et al., 2003; Wang et al., 2010).
9 We further estimate nitric acid washout scavenging coefficients by referring to field
10 measurements for particles of 10 nm (Laakso et al., 2003) and the theoretical dependence
11 of scavenging coefficients on particle sizes for particles $< 10 \text{ nm}$ (Henzing et al., 2006).
12 The collection efficiency of particles smaller than 10 nm by rain droplets is dominated by
13 Brownian diffusion, and in this regard we can treat nitric acid as a single molecule (or
14 particle) with diameter of 0.5 nm. Through this approach, we derive an empirical Λ value
15 for nitric acid of 2 cm^{-1} . In addition, we adopt the b value of 0.62 for nucleation mode
16 particles (diameter 1 nm – 40 nm) (Feng, 2007) for nitric acid. When in cloud
17 precipitation intensity is 1 mm h^{-1} , this empirical washout loss rate equals $3 \times 10^{-3} \text{ s}^{-1}$
18 which is about two orders of magnitude larger than the corresponding washout loss rate
19 ($0.1 \text{ hr}^{-1} = 2.8 \times 10^{-5} \text{ s}^{-1}$) currently in GC12.

20 For convective precipitation, MERRA2 meteorological fields do not provide
21 convective cloud fraction and water content. Therefore, the updated wet scavenging
22 method discussed above for stratiform precipitation cannot be directly applied to
23 convective precipitation rainout scavenging in GEOS-Chem. However, the empirical
24 value for nitric acid washout is also applied to convective washout in the present study as
25 Case 4.

26

27 **3. Model simulations and results**



1 To study the impacts of various updates to the wet scavenging as described in
2 Section 2 on model simulated nitric acid, nitrate, and ammonium mass concentrations, we
3 run GEOS-Chem for 4 cases: (1) standard GC12 parameterizations for rainout and
4 washout (Keller et al., 2014; Fontoukis and Nenes, 2007; Martin et al., 2003; Bey et al.,
5 2001), called GC12; (2) same as the Case GC12 except k_{new} in Eq. 3 is used, called Knew;
6 (3) same as the Case Knew except $ICCW_t$ from MERRA2 (Eq. 4) is used, called $ICCW_t$;
7 (4) same as the Case $ICCW_t$ except empirical washout rates for nitric acid and aerosols
8 are used, called $ICCW_t_{EW}$. For each case, we carry out simulations from December
9 2010 to December 2011, with the first month as spin-up. The model horizontal resolution
10 is $2^\circ \times 2.5^\circ$ and vertically there are 47 layers. The present analysis focuses on the
11 continental United States. We compared simulated nitric acid with in-situ observations at
12 Clean Air Status and Trends Network (CASTNET) sites, simulated nitrate and
13 ammonium with in-situ observations at Interagency Monitoring of Protected Visual
14 Environments (IMPROVE) and Chemical Speciation Network (CSN) sites. For 2011,
15 there were 74 sites with available nitric acid observations from CASTNET. For the same
16 year, IMPROVE had 120 sites with available nitrate and ammonium observations, while
17 CSN had 94 sites with available nitrate observations and 63 sites with available
18 ammonium observations.

19 The effects of different modifications to the GC12 wet scavenging parameterization
20 on model simulated nitric acid, nitrate, and ammonium mass concentrations are shown in
21 Figures 2-3 and Table 1. Most of the changes of mass concentrations of the 3 species over
22 the US are caused by the changes of cloud condensation variability and/or empirical
23 washout rate. The impact of new rainout loss rate (k_{new}) is relatively small because of the
24 cancelling effect of k in the denominator and also in the exponent in Eq. 1. As shown in
25 Figs. 2a-2b and Table 1, all cases except $ICCW_t_{EW}$ overestimate nitric acid at
26 CASTNET sites by a factor 2–3 in both wintertime and summertime. Consideration of
27 cloud condensation water variability slightly reduces nitric acid in January and December



1 but has negligible effect during other months. The inclusion of the empirical washout rate
2 reduces the normalized mean bias (NMB) of nitric acid from ~150 % to 24 % (Table 1).
3 Figures 2c and 2d show the impacts of improved wet scavenging on nitrate. It is clear that
4 GC12 significantly overestimates nitrate concentration at most sites especially during the
5 wintertime, in agreement with previous studies (Heald et al., 2012; Walker et al., 2012).
6 Replacing constant ICCW with variable $ICCW_t$ reduces the NMB of nitrate from 170 %
7 to 84 %. ICCW has significant impact on reducing nitrate mass concentration during the
8 wintertime and a smaller impact during the summertime. Wintertime bias of nitrate was
9 reduced from $2 \mu\text{g m}^{-3}$ to $0.7 \mu\text{g m}^{-3}$. The change of washout rate from theoretical value
10 to empirical formula results in an additional 59 % reduction of NMB for nitrate and
11 impacts nitrate mass concentration significantly both in the winter and in the summer. For
12 ammonium, NMB is reduced from 85 % to 43 % after considering rainout with variable
13 cloud condensation water. Similar to nitrate, the impact of CCW is large during the
14 wintertime and smaller during the summer time. After considering empirical washout, the
15 NMB of ammonium is reduced to 13 %. While the update in the wet scavenging
16 parameterization significantly improves agreement of the model simulated mass
17 concentrations nitric acid, nitrate, and ammonium over the US with those observed, it
18 does not affect the correlation coefficients of annual mean values (Table 1) which are
19 dominated by spatial distributions (Fig. 3).

20 Figure 3 shown the horizontal distributions of surface layer nitric acid, nitrate, and
21 ammonium mass concentrations over the US for case GC12 (a-c) and case $ICCW_t_EW$
22 (d-f). For comparison, annual mean mass concentrations observed at CASTNET,
23 IMPROVE, and CSN sites are shown in filled cycles. The spatial pattern of the simulated
24 concentrations of the three species for the $ICCW_EW$ case is close to those for the GC12
25 case. High concentrations of nitric acid are mainly located at northeastern, southern, and
26 western US with the values up to $2\text{--}4 \mu\text{g m}^{-3}$ based on GC12 (Fig. 3a) and $1\text{--}2 \mu\text{g m}^{-3}$
27 based on $ICCW_t_EW$ (Fig. 3d). Horizontal distribution of nitrate is different from that of



1 nitric acid. Nitrate is mainly located at the Ohio valley region and the Northeastern US
2 with values up to 4–5 $\mu\text{g m}^{-3}$ based on GC12 (Fig. 3b) and 1–3 $\mu\text{g m}^{-3}$ based on
3 ICCW_tEW (Fig. 3e). Ammonium shows a similar horizontal distribution to that of
4 nitrate, but its value is ~50 % lower than nitrate concentration. For the whole continental
5 US domain, the annual mean nitric acid, nitrate, and ammonium concentration in the
6 model surface layer are reduced from 1.48 $\mu\text{g m}^{-3}$ to 0.78 $\mu\text{g m}^{-3}$, 1.03 $\mu\text{g m}^{-3}$ to 0.46 $\mu\text{g m}^{-3}$,
7 0.76 $\mu\text{g m}^{-3}$ to 0.47 $\mu\text{g m}^{-3}$, respectively. The percentage changes for nitric acid,
8 nitrate, and ammonium concentrations averaged within the domain are -47%, -55%, and
9 -38%, respectively. The improved wet scavenging treatment had significant impacts on
10 nitric acid, nitrate, and ammonium modeling over the US. As can be seen from Figs.
11 3a-3f (and also Fig. 2 and Table 2), simulated nitric acid, nitrate, and ammonium mass
12 concentrations over the US based on the updated wet scavenging parameterization (i.e.,
13 ICCW_tEW) are in much better agreement with in-situ measurements.

14

15 **4. Summary and discussions**

16 We present an improved wet scavenging parameterization for use in in GEOS-Chem
17 by considering cloud condensation water variability and an empirical washout rate. The
18 updated parameterization significantly reduces the overestimation of simulated annual
19 mean mass concentrations of nitric acid, nitrate, and ammonium at CASTNET,
20 IMPROVE, and CSN sites in US, from 2.04 to 1.03 (observation: 0.83) $\mu\text{g m}^{-3}$, 1.89 to
21 0.88 (observation: 0.70) $\mu\text{g m}^{-3}$, 1.09 to 0.68 (observation: 0.60) $\mu\text{g m}^{-3}$, respectively. In
22 addition, the agreement of model simulated seasonal variations of corresponding species
23 with measurements is also improved. The updated wet scavenging scheme provides a
24 partial solution to the persistent problem of nitric acid and nitrate overestimation in the
25 widely used community model GEOS-Chem (e.g., Heald et al., 2012) and thus improve
26 the skill of the model in predicting nitric acid, nitrate, and ammonium concentrations.
27 The empirical washout rate suggested in the present work will also help to resolve the



1 significant over-prediction of nitric acid by most of the 9 global models participating in
2 the Aerosol Comparisons between Observations and Models (AeroCom) phase III study
3 (Bian et al., 2017). Due to large difference in nitric acid washout rate based on theoretical
4 and field studies and the importance of this rate, further research is needed to better
5 understand the underlying reasons and reduce the difference. At the time being, we
6 recommend the empirical values to be used in models.

7 While the present study focused on the US where abundant relevant measurements
8 are available, the updated wet scavenging parameterization impacts model simulated
9 nitric acid, nitrate and ammonium concentrations in other regions as well, particularly
10 over land. The changes of nitrate and ammonium mass concentrations not only impact
11 particle growth but also influence ammonia concentrations which are important for
12 aerosol nucleation (Kirkby et al., 2011; Yu et al., 2018), via the equilibrium of
13 sulfate-nitrate-ammonium. The updated scheme presented in this study has potential
14 implications to new particle formation, particle growth, aerosol size, CCN number
15 concentration and associated radiative forcing, which will be the subjects of future
16 research.

17

18 Code and data availability. The code of GEOS-Chem 12.0.0 is available through the
19 GEOS-Chem distribution web-page
20 http://wiki.seas.harvard.edu/geos-chem/index.php/GEOS-Chem_12. All measurement
21 data are publicly available.

22

23 Acknowledgments. This work is supported by NYSERDA under contract 100416, NASA
24 under grant NNX13AK20G, and NSF under grant 1550816. We would like to
25 acknowledge Interagency Monitoring of Protected Visual Environments (IMPROVE),
26 Chemical Speciation Network (CSN), and Clean Air Status and Trends Network
27 (CASTNET) for the in-site measurement data. GEOS-Chem is a community model



1 maintained by the GEOS-Chem Support Team at Harvard University.

2

3 **References**

4 Andronache, C., Grönholm, T., Laakso, L., Phillips, V., and Venäläinen, A., Scavenging
5 of ultrafine particles by rainfall at a boreal site: observations and model estimations,
6 *Atmos. Chem. Phys.*, 6, 4739-4754, <https://doi.org/10.5194/acp-6-4739-2006>, 2006.

7 Backes, A., Aulinger, A., Bieser, J., Matthias, V., Quante, M., Ammonia emissions in
8 Europe, part I: development of a dynamical ammonia emission inventory. *Atmos.*
9 *Environ.* 131, 55–66, 2016.

10 Bauer, S. E., Koch, D., Unger, N., Metzger, S. M., Shindell, D. T., and Streets, D. G.:
11 Nitrate aerosols today and in 2030: a global simulation including aerosols and
12 tropospheric ozone, *Atmos. Chem. Phys.*, 7, 5043-5059,
13 <https://doi.org/10.5194/acp-7-5043-2007>, 2007.

14 Beheng, K. D. and G. Doms, A general formulation of collection rates of cloud and
15 raindrops using the kinetic equation and comparison with parameterizations. *Beitr.*
16 *Phys. Atmos.*, 59, 66–84, 1986.

17 Bey, I., D. J. Jacob, R. M. Yantosca, J. A. Logan, B. Field, A. M. Fiore, Q. Li, H. Liu, L. J.
18 Mickley, and M. Schultz, Global modeling of tropospheric chemistry with
19 assimilated meteorology: Model description and evaluation, *J. Geophys. Res.*, 106,
20 23,073 – 23,096, doi:10.1029/2001JD000807, 2001.

21 Bian, H., Chin, M., Hauglustaine, D. A., Schulz, M., Myhre, G., Bauer, S. E., Lund, M. T.,
22 Karydis, V. A., Kucsera, T. L., Pan, X., Pozzer, A., Skeie, R. B., Steenrod, S. D.,
23 Sudo, K., Tsigaridis, K., Tsimpidi, A. P., and Tsyro, S. G., Investigation of global
24 particulate nitrate from the AeroCom phase III experiment, *Atmos. Chem. Phys.*, 17,
25 12911-12940, <https://doi.org/10.5194/acp-17-12911-2017>, 2017.

26 Feng, J., A 3-mode parameterization of below-cloud scavenging of aerosols for use in
27 atmospheric dispersion models, *Atmos. Environ.*, 41, 6808–6822, 2007.



- 1 Fountoukis, C., and A. Nenes, ISORROPIA II: A computationally efficient
2 thermodynamic equilibrium model for
3 $K^+-Ca^{2+}-Mg^{2+}-NH_4^+-Na^+-SO_4^{2-}-NO_3^- -Cl-H_2O$ aerosols, *Atmos. Chem. Phys.*,
4 7(17), 4639-4659, 2007.
- 5 Giorgi, F., and W. L. Chameides, Rainout lifetimes of highly soluble aerosols and gases
6 as inferred from simulations with a general circulation model, *J. Geophys. Res.*,
7 91(D13), 14367–14376, doi:10.1029/JD091iD13p14367, 1986.
- 8 Heald, C. L., Collett Jr., J. L., Lee, T., Benedict, K. B., Schwandner, F. M., Li, Y., Clarisse,
9 L., Hurtmans, D. R., Van Damme, M., Clerbaux, C., Coheur, P.-F., Philip, S., Martin,
10 R. V., and Pye, H. O. T., Atmospheric ammonia and particulate inorganic nitrogen
11 over the United States, *Atmos. Chem. Phys.*, 12, 10295–10312,
12 <https://doi.org/10.5194/acp-12-10295-2012>, 2012.
- 13 Henzing, J. S., Oliviere, D. J. L., and van Velthoven, P. F. J., A parameterization of size
14 resolved below cloud scavenging of aerosol by rain, *Atmos. Chem. Phys.*, 6,
15 3363–3375, doi:10.5194/acp-6-3363-2006, 2006.
- 16 Jacob, D. J., Liu, H., Mari, C., and Yantosca, B. M., Harvard wet deposition scheme for
17 GMI,
18 acmg.seas.harvard.edu/geos/wiki_docs/deposition/wetdep.jacob_etal_2000.pdf,
19 2000.
- 20 Keller, C. A., M. S. Long, R. M. Yantosca, A. M. Da Silva, S. Pawson, and D. J. Jacob,
21 HEMCO v1.0: A versatile, ESMF-compliant component for calculating emissions in
22 atmospheric models, *Geosci. Model Devel.*, 7, 1409-1417, 2014.
- 23 Khain, A. P. and Pinsky, M. B., Turbulence effects on the collision kernel, II: Increase of
24 the swept volume of colliding drops, *Q. J. Roy. Meteor. Soc.*, 123, 1543–1560, 1997.
- 25 Kirkby, J. and co-authors, Role of sulphuric acid, ammonia and galactic cosmic rays in
26 atmospheric aerosol nucleation, *Nature*, 476, 429–433, 2011.
- 27 Laakso, L., Grönholm, T., Rannik, U., Kosmale, M., Fiedler, V., Vehkamäki, H., and



- 1 Kulmala, M., Ultrafine particle scavenging coefficients calculated from 6 years field
2 measurements, *Atmos. Environ.*, 37, 3605–3613, 2003.
- 3 Liu, H. Y., Jacob, D. J., Bey, I., and Yantosca, R. M., Constraints from Pb-210 and Be-7
4 on wet deposition and transport in a global three-dimensional chemical tracer model
5 driven by assimilated meteorological fields, *J. Geophys. Res.-Atmos.*, 106,
6 12109–12128, 2001.
- 7 Martin, R. V., Jacob, D. J., Yantosca, R. M., Chin, M., and Ginoux, P., Global and
8 regional decreases in tropospheric oxidants from photochemical effects of aerosols, *J.*
9 *Geophys. Res.*, 108, 4097, doi:10.1029/2002JD002622, 2003.
- 10 Myhre, G., Samset, B. H., Schulz, M., Balkanski, Y., Bauer, S., Berntsen, T. K., Bian, H.,
11 Bellouin, N., Chin, M., Diehl, T., Easter, R. C., Feichter, J., Ghan, S. J.,
12 Hauglustaine, D., Iversen, T., Kinne, S., Kirkevåg, A., Lamarque, J.-F., Lin, G., Liu,
13 X., Lund, M. T., Luo, G., Ma, X., van Noije, T., Penner, J. E., Rasch, P. J., Ruiz, A.,
14 Seland, Ø., Skeie, R. B., Stier, P., Takemura, T., Tsigaridis, K., Wang, P., Wang, Z.,
15 Xu, L., Yu, H., Yu, F., Yoon, J.-H., Zhang, K., Zhang, H., and Zhou, C., Radiative
16 forcing of the direct aerosol effect from AeroCom Phase II simulations, *Atmos.*
17 *Chem. Phys.*, 13, 1853-1877, <https://doi.org/10.5194/acp-13-1853-2013>, 2013.
- 18 Park, S. H., Jung, C. H., Jung, K. R., Lee, B. K., and Lee, K. W., Wet scrubbing of
19 polydisperse aerosols by freely falling droplets, *Aerosol Sci.*, 36, 1444–1458, 2005.
- 20 Pye, H. O. T., H. Liao, S. Wu, L. J. Mickley, D. J. Jacob, D. K. Henze, and J. H. Seinfeld,
21 Effect of changes in climate and emissions on future sulfate - nitrate - ammonium
22 aerosol levels in the United States, *J. Geophys. Res.*, 114, D01205, doi:
23 10.1029/2008JD010701, 2009.
- 24 Twomey, S., The influence of pollution on the shortwave albedo of clouds, *J. Atmos. Sci.*,
25 34, 1149–1152, 1977.
- 26 Walker, J., M., Philip, S., Martin, R. V., and Seinfeld, J. H., Simulation of nitrate, sulfate,
27 and ammonium aerosols over the United States, *Atmos. Chem. Phys.*, 12,



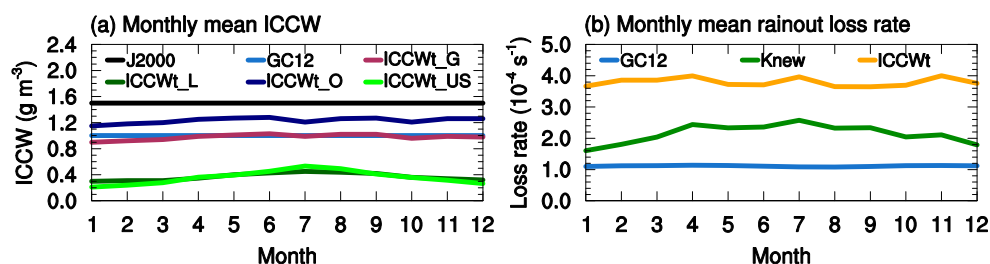
- 1 11213–11227, <https://doi.org/10.5194/acp-12-11213-2012>, 2012.
- 2 Wang, Q., D.J. Jacob, J.A. Fisher, J. Mao, E.M. Leibensperger, C.C. Carouge, P. Le Sager,
3 Y. Kondo, J.L. Jimenez, M.J. Cubison, and S.J. Doherty, Sources of carbonaceous
4 aerosols and deposited black carbon in the Arctic in winter-spring: implications for
5 radiative forcing, *Atmos. Chem. Phys.*, 11, 12,453–12,473, 2011.
- 6 Wang, X., Zhang, L., and Moran, M. D., Uncertainty assessment of current size-resolved
7 parameterizations for below-cloud particle scavenging by rain, *Atmos. Chem. Phys.*,
8 10, 5685–5705, <https://doi.org/10.5194/acp-10-5685-2010>, 2010.
- 9 Yu, F., Nadykto, A. B., Herb, J., Luo, G., Nazarenko, K. M., and Uvarova, L. A.,
10 H₂SO₄–H₂O–NH₃ ternary ion-mediated nucleation (TIMN): kinetic-based model
11 and comparison with CLOUD measurements, *Atmos. Chem. Phys.*, 18,
12 17451–17474, <https://doi.org/10.5194/acp-18-17451-2018>, 2018.
- 13 Yu, F. and Luo, G., Simulation of particle size distribution with a global aerosol model:
14 contribution of nucleation to aerosol and CCN number concentrations, *Atmos. Chem.*
15 *Phys.*, 9, 7691–7710, <https://doi.org/10.5194/acp-9-7691-2009>, 2009.
- 16 Zakoura M. and S.N. Pandis, Overprediction of aerosol nitrate by chemical transport
17 models: The role of grid resolution. *Atmos. Environ.* 187, 390–400, 2018.
- 18 Zhang, L., Jacob, D.J., Knipping, E.M., Kumar, N., Munger, J.W., Carouge, C.C., Van
19 Donkelaar, A., Wang, Y.X., Chen, D., Nitrogen deposition to the United States:
20 distribution, sources, and processes. *Atmos. Chem. Phys.* 12, 4539–4554, 2012.
- 21 Zhang, L., Michelangeli, D. V., and Taylor, P. A., Numerical studies of aerosol
22 scavenging in low-level, warm stratiform clouds and precipitation, *Atmos. Environ.*,
23 38, 4653–4665, 2004.
- 24



1 Table 1. Observed annual mean surface concentrations of HNO₃, nitrate, and ammonium
 2 at CASTNET, IMPROVE, and CSN sites. Annual mean surface concentrations (Mean),
 3 normalized mean bias (NMB), and correlation coefficient (*r*) between observed and
 4 simulated annual mean values for the 3 species by GC12, Knew, ICCW_t, and ICCW_{t_EW}
 5 cases.

	HNO ₃			NIT			NH ₄		
	Mean (μg m ⁻³)	NMB (%)	<i>r</i>	Mean (μg m ⁻³)	NMB (%)	<i>r</i>	Mean (μg m ⁻³)	NMB (%)	<i>r</i>
Observation	0.83			0.70			0.60		
GC12	2.04	145.1	0.73	1.89	168.1	0.53	1.09	81.4	0.75
Knew	2.05	146.8	0.73	1.90	170.5	0.53	1.11	84.5	0.75
ICCW _t	1.87	125.0	0.74	1.29	83.5	0.57	0.86	42.7	0.78
ICCW _{t_EW}	1.03	24.2	0.72	0.88	25.0	0.57	0.68	12.8	0.78

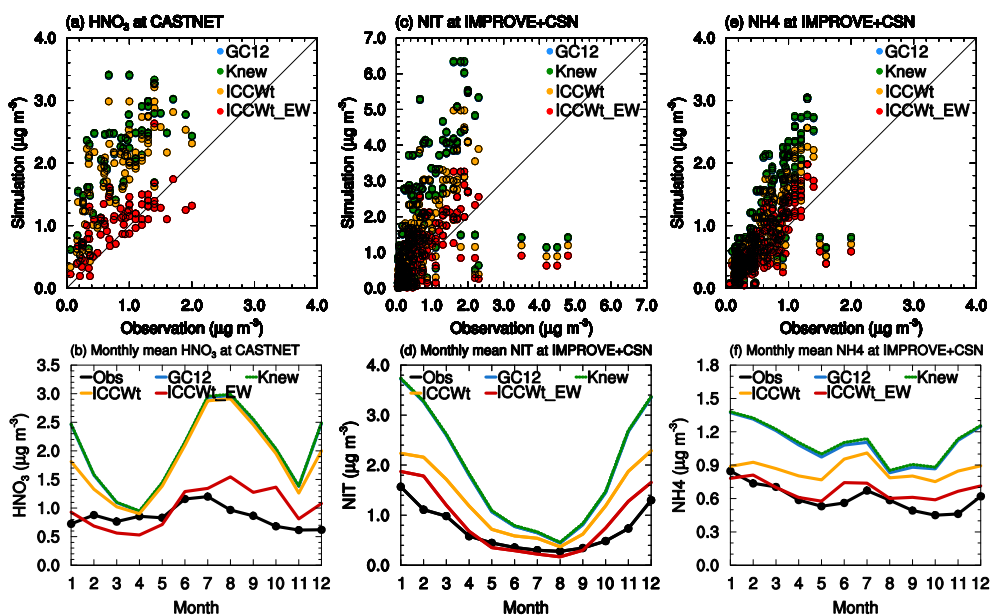
6
7
8



9

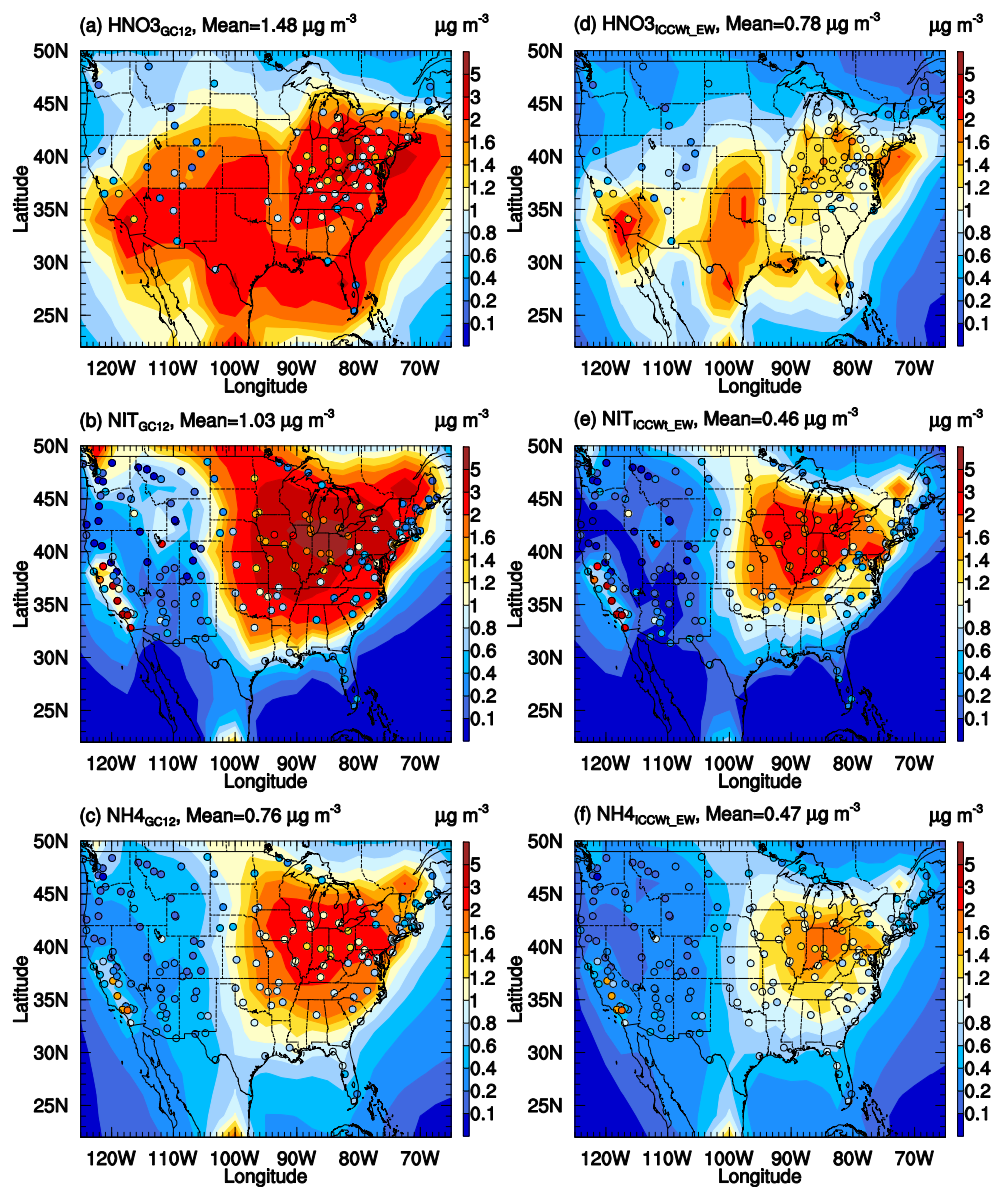
10 Figure 1. (a) Monthly variations of ICCW averaged over the lower troposphere layers of
 11 the whole globe (maroon), global land areas (olive), global oceans (navy), and
 12 continental US (green) from MERRA2, along with constant ICCW values assumed in
 13 J2000 (black) and GC12 (blue). (b) Monthly variations of the rainout loss rate averaged
 14 in the lower troposphere layers of the continental US based on Eq. (2) (i.e, GC12) and Eq.
 15 (3) with constant ICCW of 1 g m⁻³, and Eq. (3) with MERRA2 ICCW (Eq. 4).

16



1
2 Figure 2. (a) Scatter plot of observed and simulated annual mean HNO_3 at CASTNET
3 sites and (b) monthly variations of median showing the comparison between nitric acid
4 mass concentrations observed at CASTNET sites (black) and simulated by GC12 (blue),
5 Knew (green dash), ICCW_t (yellow), and ICCW_tEW (red) cases. (c) and (d) are the
6 same as (a) and (b) but for nitrate at IMPROVE+CSN sites. (e) and (f) are the same as (a)
7 and (b) but for ammonium at IMPROVE+CSN sites.

8



1

2 Figure 3. Horizontal distributions of surface layer nitric acid, nitrate, and ammonium
3 simulated by the GC12 case (a-c) and the ICCW_t_EW case (d-f). Filled circles are annual
4 mean mass concentrations observed at CASTNET, IMPROVE, and CSN for
5 corresponding species.